Physics of Atomic Nuclei, Vol. 68, No. 9, 2005, pp. 1540–1547. Translated from Yadernaya Fizika, Vol. 68, No. 9, 2005, pp. 1599–1606.

NUCLEI
Theory

Interaction of Gold Nuclei with Photoemulsion Nuclei at Energies in the Range 100–1200 MeV per Nucleon and Cascade–Evaporation Model

S. D. Bogdanov[1)], E. Ya. Shablya[1)*], S. Vokal[2)], V. F. Kosmach[1)], and V. A. Plyuschev[3)]

Received September 9, 2004; in final form, March 10, 2005

Abstract—The interaction of gold nuclei with photoemulsion nuclei at energies in the range 100–1200 MeV per nucleon was studied experimentally. A consistent comparison of the experimental data obtained in this way with the results of the calculations based on the cascade–evaporation model is performed. © *2005 Pleiades Publishing, Inc.*

INTRODUCTION

On the basis of the nuclear-photoemulsion method, the propagation of heavy (gold) nuclei through a homogeneous medium is studied here under conditions of a complete experiment in the energy range 100–1200 MeV per nucleon. Also, the features of the interactions between ^{197}Au nuclei and photoemulsion nuclei are calculated within the cascade–evaporation model [1], this including an analysis of the multiplicities of secondary particles versus the basic properties of the process. Further, our experimental data are compared with the results of the calculations.

A similar investigation of the applicability of the cascade–evaporation model to describing the interactions of lighter nuclei (Ne, Ar, Fe) with photoemulsion nuclei in the same energy range was previously performed in [2–5].

EXPERIMENT AND CALCULATIONS

In order to obtain quantitative results, we employed a photoemulsion chamber formed by 34 layers of BR-2 photoemulsion having a standard composition (3.148×10^{22} H, 1.412×10^{22} C, 0.396×10^{22} N, 0.956×10^{22} O, 0.004×10^{22} S, 0.002×10^{22} I, 1.031×10^{22} Br, and 1.036×10^{22} Ag nuclei per 1 cm^3). The dimensions of each layer were close to $10 \times 10 \times 0.05$ cm^3. The chamber was irradiated with ^{197}Au nuclei accelerated at the Bevalac accelerator (Berkeley, USA) to an energy of 1147.2 MeV per nucleon. In the irradiation, the mean fluence ranged between 500 and 2000 particles per 1 cm^2. The details of the development and primary treatment of the results obtained in the chamber are given elsewhere [6, 7].

By using the method of fast and slow scanning, 1122 tracks were traced from their entrance into the emulsion to their stop or interaction. As a result, 585 interactions of ^{197}Au nuclei over the energy range 0–1147 MeV per nucleon were found over a length of 30 m. Among these, we processed 332 inelastic interactions of ^{197}Au nuclei whose mean energy ranged between 100 and 1147 MeV per nucleon. The procedure employed here to process interactions was described in [8, 9]. In processing data on projectile disintegration, we were able to determine the charges of all projectile fragments and their polar and azimuthal emission angles.

For a sample comprising 108 inelastic interactions of ^{197}Au nuclei whose mean energy fell within the range 741.2 ± 19.8 MeV per nucleon, we measured the production angles, ionization losses, and free paths of all charged secondaries (the sample included 4444 particles).

In addition, we processed 173 nonrelativistic interactions of ^{197}Au nuclei where the atomic number of a fragment in excess of 20 was determined by the residual free path of the fragment [8], measurements for other charged particles not being performed.

The calculated statistical sample was obtained by generating the interactions between ^{197}Au nuclei of energy 700 MeV per nucleon and individual emulsion nuclei (^{1}H, ^{12}C, ^{14}N, ^{16}O, ^{80}Br, ^{107}Ag) on the basis of the Monte Carlo method and by subsequently performing summation with weights corresponding

[1)]St. Petersburg State Polytechnical University, Politekhnicheskaya ul. 29, St. Petersburg, 195251 Russia.
[2)]Joint Institute for Nuclear Research, Dubna, Moscow oblast, 141980 Russia; University of P.J. Šafárik, Jesenná 5, SK-041 54 Košice, Slovak Republic.
[3)]Khlopin Radium Institute, Vtoroĭ Murinskiĭ pr. 28, St. Petersburg, 194021 Russia.
[*]e-mail: shey79@mail.ru

to the calculated cross sections and the composition of the emulsion. In doing this, we took into account meson-production processes, a Lorentz contraction, and the effect of the Pauli exclusion principle at the fast (first) stage and the effect exerted by the change in the nuclear-matter density in the course of cascade propagation. The deexcitation of nuclear residues after the completion of the fast stage (the second stage, which is slow) is described on the basis of the statistical model. The total statistical sample obtained within the cascade–evaporation model comprised 1000 events.

INELASTIC-INTERACTION FREE PATHS OF ^{197}Au NUCLEI

On the basis of our experimental measurements, inelastic-interaction free paths of ^{197}Au nuclei in BR-2 nuclear photoemulsion were determined in the energy ranges 100–400, 400–900, 900–1200, and 100–1200 MeV per nucleon. The results obtained in this way are given in Fig. 1. Also shown in this figure are experimental results reported in [10], where Ilford-G5 emulsions and ^{197}Au nuclei were used for targets and projectiles, respectively.

Among a great variety of models for calculating cross sections for inelastic nucleus–nucleus interactions, we choose the Karol model [11] and the Bradt–Peters model [12], according to which we calculated the cross sections for the interaction of photoemulsion nuclei with ^{197}Au nuclei and the corresponding inelastic-interaction free paths for BR-2 photoemulsion in the energy range between 100 and 1200 MeV per nucleon. In this calculation, we took into account the change in the energy of the nuclei as they traverse emulsion layers and the corresponding change in the mean cross section for nucleon–nucleon interactions.

From the experimental data and from the results of the calculations (see Fig. 1), it follows that, although the cross sections for nucleon–nucleon interactions exhibit a pronounced energy dependence in the energy range being considered, the inelastic-interaction free paths of ^{197}Au nuclei in a nuclear photoemulsion are rather weakly dependent on the projectile energy. The experimental data obtained here and in [10] prove to be quite close to each other if one takes into account the distinctions between the composition and densities of BR-2 and Ilford-G5 emulsions. The calculations lead to larger cross sections for the interactions of gold nuclei and, consequently, to shorter free paths. The observed discrepancies between the calculated and measured results may be due to missing few-prong events in the experiments or to employing inaccurate values of adjustable parameters in the above models or to both of these factors.

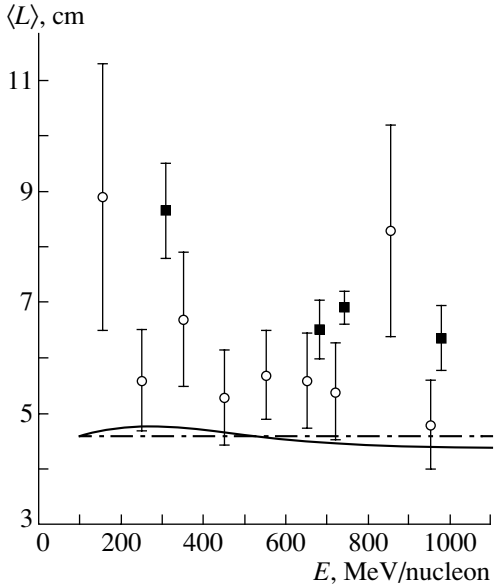

Fig. 1. Inelastic-interaction mean free paths $\langle L\rangle$ of ^{197}Au nuclei in emulsion versus the projectile energy E: (closed boxes) our present experimental data, (open circles) experimental data from [10], (solid curve) results of the calculation based on the model proposed in [11], and (dash-dotted line) results of the calculation within the model considered in [12].

MULTIPLICITIES OF SECONDARY PARTICLES

For a further analysis of our data, all secondaries were partitioned into the following groups:

(i) the group of $(g + s)$ particles defined as first-stage particles, which comprise singly charged target fragments of energy $E \geq 26$ MeV per nucleon, product mesons, and singly charged projectile fragments whose transverse momentum exceeds 222.6 MeV/c (this corresponds to $E \geq 26$ MeV per nucleon in the transverse direction);

(ii) the group of b particles defined as target fragments of energy in the range $E \leq 26$ MeV per nucleon (their free path is shorter than 3 mm), which are emitted predominantly at the second reaction stage;

(iii) the group of $(s' + g' + b')$ particles having energies in the region $E \geq 26$ MeV per nucleon and transverse momenta below 222.6 MeV/c per nucleon, this group including singly (s'), doubly (g'), and multiply (b', $Z \geq 3$) charged projectile fragments.

In each interaction event, we determined the multiplicities of particles belonging to the above groups, the total number N of charged secondaries, and their total charge $Z_{\text{int.ch.}}$ (in electron-charge units). This made it possible to obtain particle-number distributions in disintegration events induced by gold ions of energy 0.741 GeV per nucleon and correlations

Table 1. Multiplicity (in number of particles per interaction event) of charged secondaries produced in the interactions between ^{197}Au nuclei of mean energy 0.741 GeV per nucleon and photoemulsion nuclei

Interaction type	$\langle N_{g+s}\rangle$	$\langle N_b\rangle$	$\langle N_{s'+g'+b'}\rangle$	$\langle N\rangle$	$\langle Z_{\text{int.ch.}}\rangle$
^{197}Au + Em	21.71 ± 0.45	3.24 ± 0.17	16.24 ± 0.39	41.19 ± 0.62	91.97 ± 0.92
	(19.06)	(3.94)	(13.04)	(36.03)	(95.08)
^{197}Au + H	0.82 ± 0.27	0.09 ± 0.09	6.27 ± 0.76	7.18 ± 0.81	80.00 ± 2.69
	(1.34)	(0.02)	(4.14)	(5.49)	(80.02)
^{197}Au + CNO	13.39 ± 0.57	0.49 ± 0.11	20.51 ± 0.71	34.39 ± 0.92	82.51 ± 1.42
	(10.74)	(1.75)	(15.26)	(27.75)	(87.56)
^{197}Au + AgBr	31.91 ± 0.76	5.88 ± 0.32	15.07 ± 0.52	52.86 ± 0.97	101.25 ± 1.34
	(35.52)	(7.85)	(16.33)	(59.70)	(118.40)

between the numbers of different-type particles in an interaction event.

Table 1 gives the mean multiplicities of secondary particles, $\langle N_{g+s}\rangle$, $\langle N_b\rangle$, and $\langle N_{s'+g'+b'}\rangle$, and the mean multiplicity of all charged secondaries, $\langle N\rangle$, in the interactions of nuclei having various masses and energies, as well as the mean value of the total charge in an interaction event, $\langle Z_{\text{int.ch.}}\rangle$. We note that the statistical errors in the values calculated on the basis of the cascade–evaporation model (these values are given in parentheses) are approximately three times less than the experimental errors; therefore, they are not presented here.

From Table 1 and from the data obtained previously for the interactions of lighter nuclei (Ne, Ar, Fe) [2–5], it follows that an increase in the mass of colliding particles has the greatest effect on the number of particles produced at the first stage of the process. For interactions of energy below 1 GeV per nucleon, the mean multiplicity of $(g+s)$ particles is proportional to the product of the masses of interacting nuclei that is raised to a power close to 0.7, $\langle N_{g+s}\rangle \sim (A_{\text{pr}}A_{\text{tar}})^{0.7}$. Also, the total interaction charge $\langle Z_{\text{int.ch.}}\rangle$ increases with increasing dimensions of interacting nuclei. We note that $\langle Z_{\text{int.ch.}}\rangle$ does not include the target-nucleus charge, which was not detected in our experiment. The masses of interacting nuclei have a weaker effect on the mean multiplicity of all charged secondaries, $\langle N\rangle$, than on $\langle N_{g+s}\rangle$. For interactions of energy below 1 GeV per nucleon, $\langle N\rangle$ is approximately proportional to $(A_{\text{pr}}A_{\text{tar}})^{0.5}$.

As can be seen from Table 1, the results obtained by the Monte Carlo method for the mean multiplicities of $(g+s)$, b, and $(s'+g'+b')$ particles and for the mean multiplicity of all charged secondaries, as well as for the total interaction charge, are close to their experimental counterparts, describing the increase in the particle multiplicity and in $\langle Z_{\text{int.ch.}}\rangle$ with increasing mass of colliding particles.

A comparison of our experimental data with the results reported in [2, 3] revealed that the mean multiplicity of b particles is virtually independent of the projectile mass in the mass range 20–197 amu. For example, the increase in the projectile mass by a factor of 10—from that of ^{20}Ne to that of ^{197}Au—leads to only a 15% increase in the multiplicity of b particles in the interaction with heavy emulsion nuclei, the multiplicity of b particles in the interactions with light emulsion nuclei even decreasing.

In order to clarify the possible reasons behind this behavior of the multiplicity of b particles, we plotted the mean multiplicity of b particles as a function of the multiplicity of $(g+s)$ particles in disintegration events induced by the interaction between ^{197}Au nuclei of energy 0.741 GeV per nucleon and photoemulsion nuclei (see Fig. 2). Figure 2 also displays the results of the calculations based on the cascade–evaporation model that were performed for ^{197}Au nuclei of energy 0.7 GeV per nucleon and the results presented in [2, 3] for the interactions of ^{20}Ne and ^{40}Ar nuclei whose energies were, respectively, 0.28 and 0.27 GeV per nucleon.

From the data in Fig. 2, it follows that, up to a value of $N_{g+s} \approx 40$, $\langle N_b\rangle$ grows almost linearly with N_{g+s} in the interactions of gold nuclei. The emission of each of the $(g+s)$ particles (a particle that escaped from the nucleus under consideration at the fast stage) leads, on average, to an additional emission of 0.2 to 0.3 of a b particle. In the region $N_{g+s} > 40$, a decrease in the mean multiplicity of b particles with increasing multiplicity of $(g+s)$ particles is observed in disintegration events involving heavy target nuclei.

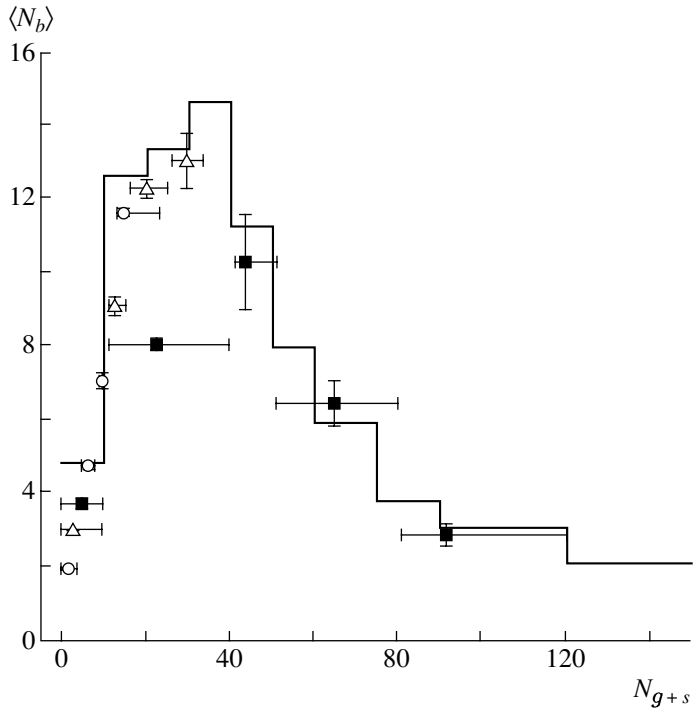

Fig. 2. Experimental correlations between the mean multiplicity of b particles and the multiplicity of fast $(g + s)$ particles in disintegration events induced by the interactions of (closed boxes) ^{197}Au nuclei of energy 0.741 GeV per nucleon, (open circles) ^{20}Ne nuclei of energy 0.28 GeV per nucleon, and (open triangles) ^{40}Ar nuclei of energy 0.27 GeV per nucleon with photoemulsion nuclei. The histogram represents the respective correlation calculated on the basis of the cascade–evaporation model for ^{197}Au nuclei of energy 0.7 GeV per nucleon.

Experiments with light projectiles of ^{20}Ne and ^{40}Ar exhibited an increase in $\langle N_b \rangle$ with increasing N_{g+s}; however, the respective correlation dependences did not show (see Fig. 2) a decrease in $\langle N_b \rangle$ as N_{g+s} grows further since there were no interactions characterized by $N_{g+s} > 40$. We also note that, in the interaction of 660-MeV protons with heavy emulsion nuclei, the number of emitted $(g + s)$ particles does not exceed three, the mean multiplicity being 1.03 particles per interaction event [12].

The simplest way to explain the observed form of the $\langle N_b \rangle (N_{g+s})$ correlation, which characterizes the interplay of the slow and the fast reaction stage, is to take into account effects that are associated with the "finiteness" of a heavy target nucleus. If the heavy target nucleus of ^{107}Ag loses 35 to 47 protons at the first reaction stage, there will be no sizable target-nucleus residue, with the result that the multiplicity of b particles will not be large. Previously, the observed effect of finiteness of a heavy target nucleus was not found in the projectile-mass range between 2 and 56 amu, since the required number of nucleons could not be knocked out of a heavy photoemulsion nucleus because of small projectile dimensions. In our opinion, the experimentally observed fact that the mean multiplicity of b particles in interactions involving light nuclei decreases as one goes over from neon to gold projectiles can also be explained by the finiteness effect. Upon undergoing a collision with gold nucleons, the bulk of the nucleons of light nuclei go over to the energy region above 26 MeV per nucleon.

The histogram in Fig. 2 represents the results of the calculations based on the cascade–evaporation model. One can easily see that this model provides a fairly good description of the complicated experimental dependence $\langle N_b \rangle (N_{g+s})$, including the experimentally observed effect of finiteness of a heavy target nucleus.

TARGET-NUCLEUS FRAGMENTATION

For each target-nucleus fragment (b particle), we determined here the polar (θ) and azimuthal (ψ) emission angles and its free path in the photoemulsion. Under the assumption that all b particles are protons, we found angular, energy, and momentum properties of each b particle. The mean values of the multiplicity ($\langle N_b \rangle$), polar emission angle, ratio of the number of particles emitted into the forward hemisphere to the number of particles emitted into the backward hemisphere (forward/backward), and longitudinal and transverse momenta ($\langle P_{||} \rangle$ and $\langle P_{\perp} \rangle$, respectively) are given in Table 2 for the interactions of gold

Table 2. Properties of target fragments of energy in the range $E \leq 26$ MeV per nucleon that are emitted at the second reaction stage

Target nucleus	$\langle N_b \rangle$, part./int.	$\langle \theta \rangle$, deg	Forward/backward	$\langle E \rangle$, MeV/nucleon	$\langle P_{\|\|} \rangle$, MeV/c	$\langle P_\perp \rangle$, MeV/c
Au, $E = 0.741$ GeV/nucleon						
Em	3.24 ± 0.17	77.81 ± 1.91	1.76 ± 0.09	9.23 ± 0.37	26.26 ± 3.92	94.96 ± 2.62
	(3.94)	(80.03)	(1.59)	(9.72)	(19.6)	(94.29)
C, N, O	0.49 ± 0.11	64.63 ± 5.14	5.67 ± 0.58	5.25 ± 1.15	36.76 ± 9.31	71.92 ± 9.15
	(1.76)	(84.30)	(1.38)	(7.24)	(13.67)	(79.02)
Ag, Br	5.88 ± 0.32	78.71 ± 2.00	1.65 ± 0.09	9.47 ± 0.38	25.43 ± 4.12	96.36 ± 2.71
	(7.85)	(79.32)	(1.62)	(10.14)	(20.54)	(96.93)
Au, $E_{\text{int}} \leq 0.873$ GeV/nucleon						
Ag, Br	5.53 ± 0.43	75.85 ± 0.23	1.77 ± 0.13	9.92 ± 0.04	30.31 ± 0.47	96.54 ± 0.30
Au, $E_{\text{int}} > 0.873$ GeV/nucleon						
Ag, Br	6.27 ± 0.49	81.62 ± 0.21	1.55 ± 0.13	9.01 ± 0.04	20.46 ± 0.43	96.17 ± 0.30

nuclei at an average energy of 741 MeV per nucleon. The results of the calculations within the cascade–evaporation model are presented in parentheses.

From Table 2, one can see that a change in the target mass by nearly a factor of 7 (in going over from C, N, and O to Ag and Br) leads to an increase in the multiplicity of b particles by almost a factor of 12, the energy by a factor of 1.8, and the transverse momentum by a factor of 1.3. Concurrently, the forward orientation becomes less pronounced—the forward/backward ratio decreases by almost a factor of 3.5, $\langle P_{||} \rangle$ decreases by a factor of 1.5, and the polar emission angle increases by a factor of 1.2.

The results of the calculations within the cascade–evaporation model are in satisfactory agreement with the experimentally determined properties of b particles in interactions with heavy photoemulsion nuclei, the discrepancies being within 5 to 10%. The calculations describe qualitatively the dependences of the multiplicity, energy, and transverse momentum of low-energy protons on the target-nucleus mass.

In order to analyze the effect of the projectile velocity on the properties of b particles, the entire body of data on interactions with heavy photoemulsion nuclei was partitioned into two groups where the interaction energies were $E_{\text{int}} \leqslant 873$ MeV per nucleon and $E_{\text{int}} > 873$ MeV per nucleon (samples containing identical numbers of b particles). The properties of b particles belonging to these samples are also given in Table 2. One can see that, with decreasing projectile velocity, the forward orientation of b particles becomes more pronounced, the longitudinal momentum component increasing by a factor of 1.5. The mean emission angle decreases by 20%. This effect was previously observed in [2–5], where it was explained by the contribution of first-stage particles to the energy region $E < 26$ MeV per nucleon, this contribution increasing as the projectile energy decreases.

The measurements of the free paths and of the azimuthal and polar emission angles in our experiment made it possible to determine the 3-momentum components for each of the b particles. For our analysis, we choose $P_z(P_{||})$, which is the momentum component along the direction of projectile motion, and $P_x(P_\perp \cos\psi)$, which is the projection of the momentum onto an axis in the azimuthal plane that is orthogonal to the direction of projectile motion.

In Fig. 3, we present the results obtained for the distributions of b particles with respect to these 3-momentum components from our measurements (Figs. 3*a*, 3*c*) and from the calculations within the cascade–evaporation model (Figs. 3*b*, 3*d*). Both the experimental and the measured distributions are close to Gaussian distributions, this giving sufficient grounds to consider a system that emits particles isotropically and which has a characteristic temperature and moves at a specific velocity. The effective temperature of the system emitting particles can be estimated by assuming that the distribution of singly charged particles with respect to each 3-momentum component is described by a Gaussian distribution characterized by the parameter $\sigma = (2/\pi)^{0.5}\langle P_\perp \rangle$, the variance being related to the temperature by the equation $T_0 = \sigma^2/m$. Both for the experimental events and for their counterparts calculated within the cascade–evaporation model, the estimates performed

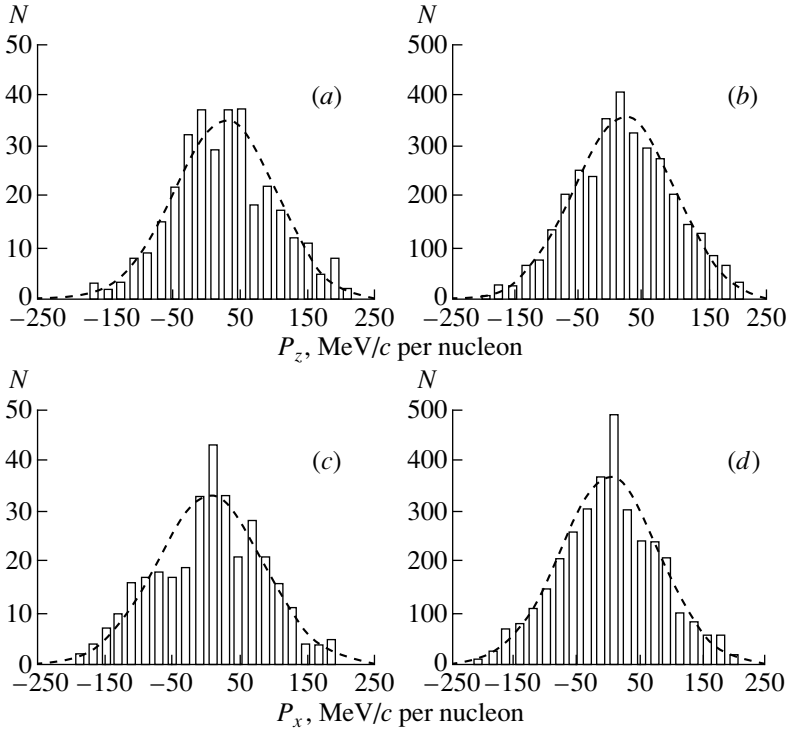

Fig. 3. Distributions of b particles with respect to two 3-momentum components (P_z, P_x) in the interactions of ^{197}Au nuclei with photoemulsion nuclei at an average energy of 0.741 GeV per nucleon. The histograms represent experimental data in Figs. 3*a* and 3*c* and the results of the calculations within the cascade–evaporation model in Figs. 3*b* and 3*d*. The dashed curves correspond to approximations by a Gaussian distribution.

for the interaction with heavy nuclei yield a value of about 6 MeV for the effective particle-emission temperature and a value of $\langle\beta_{||}\rangle = 0.025$ of the speed of light for the velocity in question.

PROJECTILE-NUCLEUS FRAGMENTATION

For the interactions of gold nuclei with photoemulsion nuclei at an average energy of 741 MeV per nucleon, Table 3 gives the mean multiplicities of doubly and multiply charged fragments ($\langle N_{g'}\rangle$ and $\langle N_{b'}\rangle$, respectively), the mean multiplicities of multiply charged fragments in various charge intervals (columns 4–6), and the mean charge of $Z \geq 3$ fragments ($\langle Z_{\mathrm{fr}}\rangle$). The respective values obtained from the calculations within the cascade–evaporation model are presented in parentheses.

From an analysis of the data in this table on the multiplicity of b' particles, one can easily see that there are two regions both in the calculated data and in the experimental data at $E \approx 700$ MeV per nucleon: these are the region of fragment charges close to the projectile charge ($Z = 61$–79), where the calculated values exceed considerably their experimental counterparts, and the fragment-charge region $Z = 3$–20, where the calculation predicts fragment yields below the experimental data. By way of example, we indicate that, in the first region, the adequate calculated data for our statistical sample (1000 events) at a projectile energy of about 700 MeV per nucleon should have been only 180 fragments instead of 590 actually obtained in the calculation—that is, the discrepancy in this region of fragment atomic numbers is as great as a factor of 3. In the region $Z = 3$–20, the experimental data differ from the results of the calculations by a factor of 18.

The data that we obtained show that the model applied here is unable to take adequately into account the multifragmentation and fission of excited heavy nuclear residues. As a result, the calculations involve virtually no interactions leading to the emission of two or more heavy fragments. The mean multiplicity of heavy fragments of the incident nucleus ^{197}Au was 1.7 to 2.7 particles per interaction event in the experiment (see Table 3), whereas its calculated value amounted to unity. An increase in the probability of the multifragmentation and fission of excited projectile fragments within the model would lead to an increase in the multiplicity of fragments in the range $Z = 3$–20 and would increase, by and large, the multiplicity of $Z \geq 3$ fragments in the interactions of nuclei, and this would make it possible to describe the experimental data more adequately.

Table 3. Multiplicity of multiply charged projectile fragments formed in the interaction of ^{197}Au nuclei with photoemulsion nuclei at an average energy of 0.741 GeV per nucleon

Target nucleus	$\langle N_{g'} \rangle$, part./int.	$\langle N_{b'} \rangle$, part./int.	Intervals in Z			$\langle Z_{\mathrm{fr}} \rangle$, el. ch.
			3–20	21–60	61–79	
Em	4.76 ± 0.21	2.52 ± 0.15	1.74 ± 0.13	0.62 ± 0.08	0.16 ± 0.04	18.79 ± 0.26
	(1.97)	(1.00)	(0.08)	(0.35)	(0.57)	(58.10)
H	2.27 ± 0.46	1.73 ± 0.40	0.27 ± 0.16	1.09 ± 0.31	0.36 ± 0.18	41.53 ± 1.48
	(0.91)	(1.00)	(0.00)	(0.03)	(0.97)	(74.70)
C, N, O	5.83 ± 0.38	3.37 ± 0.29	2.68 ± 0.26	0.63 ± 0.12	0.05 ± 0.03	13.38 ± 0.31
	(2.52)	(1.00)	(0.06)	(0.39)	(0.56)	(57.66)
Ag, Br	4.46 ± 0.28	2.05 ± 0.19	1.34 ± 0.15	0.52 ± 0.10	0.21 ± 0.06	21.51 ± 0.43
	(2.14)	(1.00)	(0.14)	(0.51)	(0.35)	(49.04)

In order to separate fission events from the whole array of processed events of ^{197}Au disintegration at an energy of 0.741 GeV per nucleon, we selected four events that involved at least two fast projectile fragments carrying $Z_{\mathrm{fr}} \geq 20$ elementary charge units each. Thus, the ratio of the cross section for the formation of two massive fragments to the total inelastic cross section was 0.037 ± 0.010, which is close to the probability of the binary fission of ^{197}Au nuclei that is induced by high-energy protons (3–5% [12]).

CONCLUSION

New experimental and calculated data have been obtained for inelastic-interaction free paths of ^{197}Au nuclei in photoemulsion and for the multiplicities of various charged secondaries produced in the inelastic interaction of gold nuclei with photoemulsion nuclei at energies in the range 100–1147 MeV per nucleon, as well as for the angular, energy, and momentum properties of these particles. The fragmentation of target and projectile nuclei has been considered. The properties of the interaction have been analyzed versus the energy of interacting nuclei.

For particles emitted at the slow stage, we have discovered the effect of finiteness of heavy photoemulsion nuclei in their interaction with gold ions. This effect was not observed previously in the projectile-mass range between 2 and 56 amu. The behavior of particles originating at the second stage of the process from target nuclei can be described quite accurately within the model of a thermalized source that emits particles isotropically and which has an effective temperature of about 6 MeV and moves at a velocity of $\langle \beta_{||} \rangle = 0.025$ of the speed of light.

In studying projectile fragments, we have found that the main discrepancy between the calculated and experimental data consists in that the calculation underestimates significantly the probability of the disintegration of a fast nucleus into several $Z \geq 3$ fragments, with the result that the charge spectra of ^{197}Au fragments appear to be distorted. Otherwise, the results of the calculations within the cascade–evaporation model describe qualitatively and quantitatively (to within 10 to 15%) our experimental data, including correlation dependences and the angular, energy, and momentum features of charged secondaries versus the target mass and particle type.

ACKNOWLEDGMENTS

We are grateful to the personnel of the Bevatron in Berkeley and the staff of the Laboratory of High Energies at the Joint Institute for Nuclear Research (JINR, Dubna), who prepared photoemulsion data and placed them at our disposal.

REFERENCES

1. S. D. Bogdanov, S. S. Bogdanov, V. F. Kosmach, *et al.*, Izv. Akad. Nauk, Ser. Fiz. **60**, 132 (1996).
2. V. E. Dudkin, E. E. Kovalev, N. A. Nefedov, *et al.*, Nucl. Phys. A **568**, 906 (1994).
3. S. D. Bogdanov, V. F. Kosmach, V. M. Molchanov, and V. A. Plyushchev, Izv. Akad. Nauk, Ser. Fiz. **63**, 427 (1999).
4. V. A. Bakaev, S. D. Bogdanov, S. S. Bogdanov, *et al.*, Izv. Akad. Nauk, Ser. Fiz. **64**, 2144 (2000).

5. S. D. Bogdanov, S. S. Bogdanov, V. E. Dudkin, *et al.*, Nucl. Tracks Radiat. Meas. **25**, 111 (1995).
6. S. D. Bogdanov, S. S. Bogdanov, E. E. Zhurkin, and V. F. Kosmach, Zh. Éksp. Teor. Fiz. **115,** 404 (1999) [JETP **88**, 220 (1999)].
7. V. A. Bakaev, S. D. Bogdanov, S. S. Bogdanov, *et al.*, Surf. Inv. **13**, 681 (1998).
8. V. A. Bakaev, S. D. Bogdanov, S. S. Bogdanov, *et al.*, Poverkhnost, No. 4, 41 (2003).
9. V. A. Bakaev, S. D. Bogdanov, S. S. Bogdanov, *et al.*, Poverkhnost, No. 4, 45 (2004).
10. C. J. Waddington and P. S. Freier, Phys. Rev. C **31**, 888 (1985).
11. P. J. Karol, Phys. Rev. C **11,** 1203 (1975).
12. V. S. Barashenkov and V. D. Toneev, *Interactions of High-Energy Particles and Nuclei with Nuclei* (Atomizdat, Moscow, 1972) [in Russian].

Translated by A. Isaakyan